Impacts of land use and land cover changes on evapotranspiration and runoff at Shalamulun River watershed, China

Xiaoli Yang, Liliang Ren, V. P. Singh, Xiaofan Liu, Fei Yuan, Shanhu Jiang and Bin Yong

ABSTRACT

The study assesses the effect of land use and land cover changes (LUCC) on evapotranspiration and runoff in the Shalamulun River watershed of 2,453 km^2 located in Inner Mongolia Autonomic Region of China. First, Landsat Thematic Mapper (TM) and Enhanced Thematic Mapper Plus (ETM+) images from 1987, 2001 and 2007 are used to quantify LUCC in the watershed. A knowledge-based decision tree (K-DT) classification technique is used to detect LUCC. By comparison of post-classification change among 1987, 2001 and 2007, the results showed significant modification and conversion of land use and cover of the watershed over the 20-year period 1987–2007. The results show that the forest area underwent the greatest change, decreasing by 159.2 km^2 in the study period. At the same time, the area of farmland, barren land and residential land increased by 89.5, 46.4 and 25.3 km^2, respectively. Subsequently, a two-source potential evapotranspiration (PET) model is used to estimate the potential evapotranspiration response to LUCC. Finally, the influence of LUCC on annual runoff is evaluated using a statistical method. LUCC potentially caused a decrease in annual PET and runoff. Meanwhile, the land use changes resulted in spatio-temporal variations of monthly PET in the growing season (April–September).

Key words | headwater, knowledge-based decision tree, land cover change, land use change, potential evapotranspiration

Xiaoli Yang (corresponding author)
Liliang Ren
V. P. Singh
Xiaofan Liu
Fei Yuan
Shanhu Jiang
Bin Yong
State Key Laboratory of Hydrology-Water
    Resources and Hydraulic Engineering,
Hohai University,
No. 1 Xikang Road,
Nanjing 210098,
China
E-mail: rll@hhu.edu.cn

INTRODUCTION

Land use and land cover changes (LUCC) are among the most hydrologically important alterations of the Earth's land surface (Diouf & Lambin 2001). LUCC is emerging as a key environmental issue and is a major factor for global change, providing scenarios for global and regional models of climate change and land-ecological systems and helping to understand interactions in the human-land system (Hovius 1998). For this reason, LUCC is treated as a core joint project of the International Geosphere Biosphere Program (IGBP) and International Human Dimensions Program on Global Environmental Change (IHDP) (Xiao et al. 2006). Information on the actual

land use and land cover (LULC) is necessary for the accurate description of many physical processes taking place on Earth's surface (Bach et al. 2006). Thus, land use and land cover maps are used in model applications to describe the spatial allocation and pattern of land use and land cover and to estimate aerial extent and location of various cover classes (Stehman & Czaplewski 1998).

Arid and semi-arid regions play an important role in the system of global change. In semi-arid regions, land cover modifications i.e. subtle changes that affect the characteristics of the land cover without changing its overall

classification, are common (Diouf & Lambin 2001). Many studies have discussed land use and land cover changes in arid and semi-arid regions (Langley *et al.* 2001; Stefanov *et al.* 2001; Govers *et al.* 2006; Wei *et al.* 2007). However, these results cannot be applied to all arid and semi-arid regions, because the regional land-use pattern is a combination of various land use types and the conversion among different land use types is complex.

In semi-arid regions, the water resources of a river basin are significantly impacted by decadal or inter-decadal climate variability, changes in land use and land cover in the upstream basin, construction of large artificial lakes and diversion of water for irrigation (Costa *et al.* 2003). Furthermore, rainfall patterns in semi-arid regions are unpredictable in both space and time. Consequently, the ability to successfully manage the resulting runoff is extremely important (Bellot *et al.* 2001; Winnaar *et al.* 2007). Evapotranspiration (ET) and runoff are amongst the most important key components in the hydrological cycle, which are closely related to LUCC. Potential evapotranspiration (PET) is generally considered to be the amount of water that is lost to the atmosphere from a land surface with ample water supply. It is one of the most complicated variables in the coupled eco-hydrology system, mainly due to its high spatio-temporal variability (Zhao *et al.* 2004). Land use change directly impacts the evapotranspiration regime; likewise, the degree and type of ground cover has an enormous impact on the initiation of surface runoff (Fohrer *et al.* 2001). As hydrological processes vary both temporally and spatially, it is common to employ remote sensing (RS) and geographical information system (GIS) tools in hydrologic modelling.

In this study, a two-source PET and statistics method supported by RS and GIS techniques were used to analyse the impact of land use and land cover changes on PET and runoff at Shalamulun River watershed. The objectives of this study were to: (1) provide a recent perspective on the spatial and temporal LULC patterns; (2) analyse land use and land cover changes that have taken place in the headwaters from 1987 to 2007; and (3) assess, quantitatively, the impact of past land use change on the PET and discharge in semi-arid regions, based on long-term historical data from Shalamulun River watershed.

STUDY AREA

The Shalamulun River is a headwater of the West Liao River with an area of approximately 2,453 km^2 located in a semi-arid region. It is situated in Inner Mongolia Autonomous Region, in the northeast of China, extending between 42°30′ and 43°15′ N and 116°40′ and 117°35′ E (Figure 1). The land use of the area is dominated by grassland, forest and farmland. The area comprises a variety of landforms ranging from grass plains to hills encompassing valleys and uplands with elevation ranging from approximately 1,000 m above sea level near Henanyingzi station to in excess of 2,000 m on the eastern border of the watershed. The climate in the study area is semi-arid and semi-humid, with an average annual precipitation of 360 mm (mean monthly rainfall varying from 2 mm in January to 108 mm in July) and annual average maximum (minimum) temperature is 5–7 °C ranging from −11 to −13 °C in January to 25 °C in July. There is a small rainfall gradient across the watershed increasing from south to north, reflecting higher topography in the south.

DATA UTILIZED

Remote sensing images

Three bitemporal clear, cloud-free Landsat Thematic Mapper (TM) and Enhanced Thematic Mapper Plus (ETM+) images for three different dates (21 June 1987, 6 July 2001 and
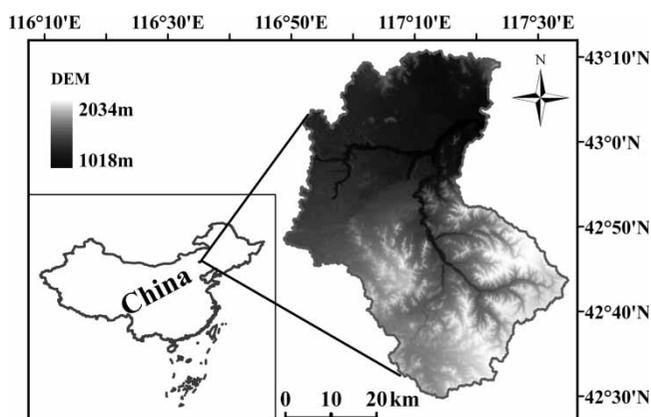

Figure 1 │ Location map of the Shalamulun River watershed.

7 October 2007) were selected to classify land use and land cover of the study area (Path 123, Row 30). The data have a 30 m ground resolution (except for the thermal IR band 6, which has a 120 m resolution) and seven spectral bands.

Leaf area index (LAI) data

In this study, 8-day LAI production of MODerate Resolution Imaging Spectroradiometer (MODIS) data at 1,000 m resolution from 2001 and 2007 were acquired from the Earth Observation Satellite (EOS) data gateway (https://wist. echo.nasa.gov/apimalized). As no 8-day LAI production of MODIS data are available before 2000, LAI from 1987 was retrieved from the Normalized Difference Vegetation Index (NDVI) from the national Oceanic and Atmospheric Administration-Advanced Very High Resolution Radiometer (NOAA-AVHRR) using the Simple Biosphere Model 2 (SiB2) method.

Meteorological data

Meteorological data from 1987 to 2007 at the Chifeng and Weichang meteorological stations were obtained from the China Meteorological Administration. The data included daily readings of mean, maximum and minimum temperatures, sunshine hours, wind speed and air water vapour pressure every 6 h.

Digital elevation model (DEM) data

The Shuttle Radar Topography Mission (SRTM) 3-second digital elevation model (DEM) data (http://lpdaac.usgs. gov/gtopo30/hydro/index.html) were used to represent the topography of the study area. The basin part of the DEM is clipped out in ArcGIS 9.2 software using the basin boundary, which is acquired from the Rivertools 2.4 software.

Digital soil type data

The digital soil map (Figure 2) covering the study area was established using ARCGIS 9.2 and showed the presence of five soil classes: aeolian soils, black soils, chernozems, dark castanozems and grey forest soils.
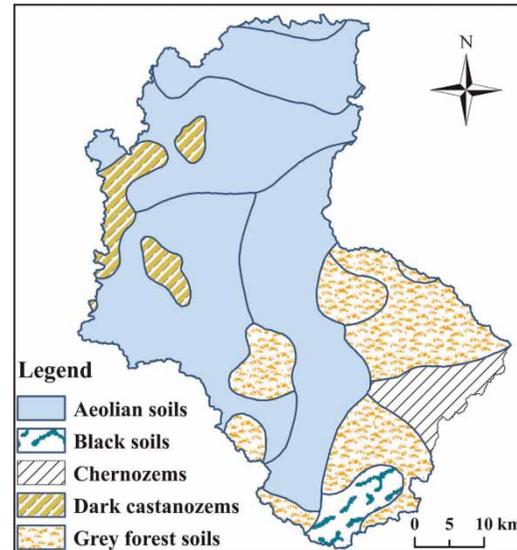

Figure 2 | Soil map of the Shalamulun River watershed.

Other ancillary data

Some ancillary data were available including 1:100,000 topographic maps, statistical records and land resources survey reports. Field surveys for the study area were conducted in August 2008. Nearly 100 Global Position System (GPS) points were located, photographed and described. During field data collection, details of the land cover as well as land use were recorded; a mobile mapping system equipped with a palm top and GPS was used to record location.

METHODS

Image pre-processing

Images acquired at different times usually have different errors for the haze and dust in the atmosphere (Berberoglu & Akin 2009). Meanwhile, there are potential non-systematic or random distortions present in the remote sensing data. These errors lead to an overestimation or low estimate of actual land use and land cover change (Stow 1999). In order to eliminate these differences and errors, the three dates of remote sensing images used in our study were corrected for atmospheric and geometric effects as follows.

An image-based technique developed by Chavez (1996) known as the Cosine(t) (COST) mode was applied to eliminate the atmospheric differences. All images were acquired in the Mercator projection (Universal Transverse Mercator projection, UTM) zone 50, World Geodetic System GPS (WGS) 84, and the geometric correction was performed on all the images using ground control points established with GPS units on site from survey land use data in 2008. The two TM images of 1987 and 2007 were co-registered to the 2001 ETM+ image. The root mean square errors were less than 0.45 pixels (12.8 m) for each of the images.

All pre-processing steps were performed using the image processing computer software ENVI, version 4.5. The scenes were subset using UTM coordinates located outside of the range boundaries for the basin boundary acquired form DEM to clip out identical areas of interest from each scene.

The basin part of the Hydro1K DEM was clipped out in ArcGIS 9.2 software using the basin boundary, which is acquired from the Rivertools 2.4 software. Furthermore, the slope and elevation data were derived from the DEM as natural factors of land use and land cover change.

The Normalized Difference Vegetation Index (NDVI) index provides an estimate of vegetation density with a ratio of visible red to near-infrared reflectance (NIR) calculated directly from the TM/ETM+ bands, which is added as an additional index band to improve sensitivity to forest structural and other land use and land cover categories (Sesnie *et al.* 2008). NDVI is often regarded as an effective method to enhance the difference between spectral features and suppress topography and shade (Berberoglu & Akin 2009).

In order to increase the accuracy of land use and land cover classification of the three images, some image transformations was used. These image transformations can enhance the difference among spectral features and include Tasseled Cap Transformation (TCT), Minimum Noise Fraction (MNF) rotation and Principal Component Analyses (PCA).

In this study, all images such as DEM, soil type map, etc. were averaged into a 28.5×28.5 m grid cell size using a nearest-neighbour method to match Landsat TM pixel size during the process of land use and land cover change detection. All the images were then resized to 300×300 m using

the same method when modelling the PET for the limit of the computer software and hardware.

Classification of land use and land cover

In spite of the progress made in simulation techniques and data acquisition, uncertainty levels remain high and the predictability of land use and land cover changes in most instances remain low (Pontius *et al.* 2008), indicating the need to further improve our understanding and characterization of land change (Verburg *et al.* 2009). Among the various methods, Geographical Information Systems (GIS) and Remote Sensing (RS) are powerful and cost-effective tools for assessing the spatial and temporal dynamics of LULC. Remote sensing data provide valuable multi-temporal data on the processes and patterns of land use and land cover change, and GIS is useful for mapping and analysing these patterns (Zhang *et al.* 2002). RS and GIS are therefore commonly integrated in detecting and monitoring land cover change at various scales with useful results (Stefanov *et al.* 2001; Hathout 2002; Lambin *et al.* 2003; Serra *et al.* 2008; Dewan & Yamaguchi 2009). Traditional approaches to automated land cover mapping using remotely sensed data have employed pattern recognition techniques, including both supervised and unsupervised approaches (Richards 1992). More recently, techniques such as expert systems, decision tree and neural networks have been used (Wharton 1989; Benediktsson *et al.* 1990).

Decision tree (DT) classification techniques are suitable for remote sensing classification problems because of their flexibility, intuitive simplicity and computational efficiency, which has led to increased acceptance (Pal & Mather 2003). A knowledge-based system built on the Dempster–Shafer theory of evidence (D–S ToE) (Shafer 1976) has long been recognized to be able to handle multi-source datasets (Peddle 1995) for a variety of classification tasks (Cohena & Shoshany 2005). An important feature of the D–S ToE is its ability to function well despite incomplete, missing and conflicting evidence (Hégarat-Mascle *et al.* 1997) by incorporation of multi-source information when computing the accumulated evidential support for each inferred class at each image pixel. Furthermore, this method of integrating geographical knowledge (including

spectral and geospatial information such as elevation, slope, aspect, etc.) is accurate and efficient for land cover classification in remote sensing (Kandrika & Roy 2008).

In order to obtain a relatively higher detection accuracy of the land use and land cover classification, a knowledge-based decision tree classification (K-DT) method was used in this study. The K-DT is a kind of decision tree classification incorporating multi-source information and expert knowledge for computing accumulated evidential support for each inferred class at each image pixel. A K-DT includes a root node (containing all data), a set of internal nodes (splits) and a set of terminal nodes (leaves). Each node makes a binary decision by carrying maximum information automatically selected for one class or some of the classes from the remaining classes. At each node, a decision rule is required and this point can be implemented using a splitting test:

$$\sum_{i}^{n} a_i x_i \leq c \quad \text{or} \quad x_i > c \qquad (1)$$

where the former equation is for multivariate decision trees and the latter for univariate decision trees; x_i represents the measurement vectors on the n selected features and a is a vector of linear discriminate coefficients while c is the decision threshold (Brodley & Utgoff 1992).

On the basis of a Chinese land use and land cover classification system (Liu 1996) developed by the Institute of Geographical Science and Natural Resources Research, Chinese Academy of Sciences (CAS), and considering the specific land use of the Shalamulun River watershed, a classification scheme with six classes of land use and land cover is proposed: grassland, forest, barren land, farmland, residential land and water body. In theory, every geographical object has proper spectral features. Based on this characteristic, the ground element can be interpreted automatically. According to the field survey data and the characteristic of six land use classes in the TM/ETM+, 30 training areas were selected in each land use type to analyse the spectral characteristic (Figure 3). Other information including elevation, percent slope, normal difference vegetation index (NDVI), image texture and previous land use data was integrated. Imagery was processed using an 'expert system' approach, whereby each pixel was evaluated using a series of decision rules (DeFries *et al.* 1998). All the
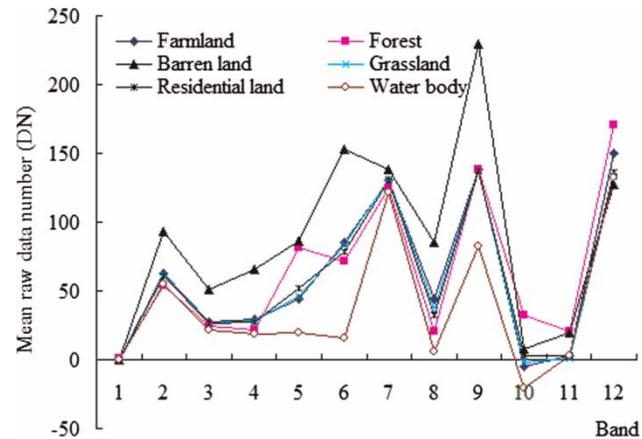

Figure 3 │ Mean spectrum of samples of different land use and land cover classes. 1–7: TM band of TM; 8: brightness of TCT; 9: greenness of TCT; 10: third of TCT; 11: slope; and 12: elevation (×10).

rule sets were imported into ENVI 4.5 and the entire image dataset has been classified.

Detection of land use and land cover changes and assessment of accuracy

There are many techniques available to detect and record differences (e.g. image differencing, ratios or correlation) and these might be attributable to change (Shalaby & Tateishi 2007). Post-classification comparison proved to be the most effective technique because data from two dates were separately classified, thereby minimizing the problem of normalizing for atmospheric and sensor differences between two dates (Shalaby & Tateishi 2007). In this study, land use and land cover data generated with K-DT classifiers from 1987 and 2001 Landsat TM and 2007 ETM+ images were used to quantify changes using a pixel-by-pixel post-classification comparison.

Assessment of accuracy is an important part of classification and detection of change (Lu *et al.* 2005). Error matrices as cross-tabulations of the mapped class versus the reference class were used to assess the accuracy of the classification (Congalton & Green 1999). Overall accuracy, user's and producer's accuracies and the Kappa statistic were then derived from error matrices. The Kappa statistic incorporates the off-diagonal elements of error matrices (i.e. classification errors) and represents the agreement obtained after removing the proportion of agreement that could be expected to occur by chance (Yuan *et al.* 2005).

In this study, an independent sample of an average of 100 polygons was randomly selected from each classification to assess classification accuracies.

Influence of land use and land cover on water cycle

In this study, the influence of LUCC on PET and annual runoff were quantitatively analysed through a physically-based two-source potential evapotranspiration (PET) model and a statistical method of analysis for the Shalamulun River watershed. The physically based two-source PET model was modified by Yuan *et al.* (2008) based on the two-source ET model (Mo *et al.* 2004). It is a distributed physically-based model that is able to calculate PET on each grid cell considering the LULC characteristics. This method was applied successfully in the Laohahe Watershed, which is much closed to the Shalamulun watershed (Ren *et al.* 2009). The model can calculate the PET consisting of potential canopy transpiration, potential soil evaporation and direct evaporation from the intercepted water:

$$E_c = \frac{\Delta R_{nc} + (\rho C_p D_0 / r_{ac})}{\lambda[\Delta + \gamma(1 + (r_c/r_{ac}))]}(1 - W_{fr}) \qquad (2)$$

$$E_{pc} = \frac{\Delta R_{nc} + (\rho C_p D_0 / r_{ac})}{\lambda[\Delta + \gamma(1 + (r_{cp}/r_{ac}))]}(1 - W_{fr}) \qquad (3)$$

$$E_{ps} = \frac{\Delta(R_{ns} - G) + (\rho C_p D_0 / r_{as})}{\lambda[\Delta + \gamma(1 + (r_{sp}/r_{as}))]} \qquad (4)$$

where E_c is the canopy transpiration, E_{pc} is the potential canopy transpiration and E_{ps} is the potential soil evaporation; R_{nc} and R_{ns} are the net radiation absorbed by canopy and soil (W m^{-2}) respectively; G is the soil heat flux (W m^{-2}); λ is the latent heat of vaporization (MJ kg^{-1}); ρ is the air density (kg m^{-3}); C_p is the air specific heat at constant pressure (KJ kg $^{\circ}$C^{-1}); γ is the psychrometric constant (kPa $^{\circ}$C^{-1}); Δ is the first-order derivative of saturation vapour pressure with temperature (kPa $^{\circ}$C^{-1}); W_{fr} is the wetted fraction of the canopy; r_{ac}, r_{cp}, r_{sp} and r_{as} are the bulk boundary-layer resistance of the canopy, the bulk stomatal resistance of canopy with the soil moisture at field capacity, the soil surface resistance with the soil moisture at field capacity and the aerodynamic resistance

between the soil surface and canopy air space, respectively (s m^{-1}); and D_0 is the water vapour deficit at the source height (kPa).

RESULTS

Land use and land cover classification

Error matrices were used to assess the accuracy of classification of LUCC. For 1987, 2001 and 2007, the overall accuracies were 85.7, 89.4 and 87.9%; the Kappa statistic was 87.4, 89.2 and 87.6%, respectively. User's and producer's accuracies of individual classes were consistently higher than 90%. These indices can meet the lowest demand for detection of change (Lucas *et al.* 1989). In this study the different spectral characteristics of TM5 and NDVI and elevation in Figure 3 is used to distinguish the forest and natural and artificial forest land use types. In particular, areas around garden trees and residential land have low slope and are more regularly shaped than natural and artificial forest, allowing us to distinguish the two land use types. Farmland has higher soil moisture and higher vegetation density affecting drainage and nutrient mineralization rates, which can be evident from pixel values of TCT and NDVI. A mean textural occurrence filter has been shown to improve spectral separation between farmland and grassland, as farmland has spectral boundaries.

Misclassifications occur mainly due to confusion between grassland and forest and between farmland and residential land. This situation can be explained by the fact that the grassland and farmland have similar spectral characteristics, if the crop is millet. Furthermore, many parts of farmland have the same elevation, slope and moisture as these farmlands are fallow fields reclaimed from grassland. There is also spectral confusion between residential areas and the forest class, because houses are surrounded by gardens and there are many trees alongside roads.

The land use and land cover maps for 1987, 2001 and 2007 were produced from Landsat TM/ETM+ images, as shown in Figure 4. From this figure, it can be found that grassland is the principal land cover type in the study area. The grassland area accounted for 66–70% (the largest of
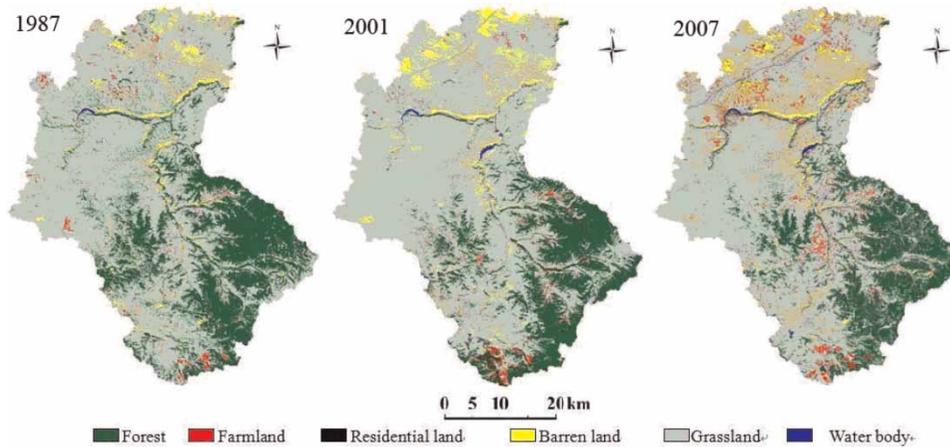
Figure 4 | Land use class maps of Shalamulum River watershed in 1987, 2001 and 2007.

Land use and land cover change

The land use and land cover change for the study area are presented in Table 1. It is clear that there has been a considerable land use and land cover change during the period 1987–2001. The most obvious land use changes that occurred in the category of forest decreased by about 155.3 km^2 (6.3% of the total area), which is an average of more than 11 km^2 yr^{-1}. The grassland areas were increased by about 80.5 km^2. During the same period, farmland areas increased in size by 18.9 km^2. The residential land and water body underwent a slight increase of about 0.5 and 3.9 km^2, respectively. During the period 2001–2007, forest land decreased and the residential land and farmland increased due to the reduction of grassland. The changed

residential land, farmland, grassland and forest areas were 24.8, 70.6, 85.4 and 3.92 km^2, respectively.

Comparing the two sub-periods (1987–2001 and 2001–2007), it can be seen that the land use and land cover changes have non-uniform characteristics. There is a larger increase of farmland during the second stage (70.7 km^2) than the first stage (18.9 km^2). The increase of residential land in the second stage was about 50 times that of the first stage. Thus, the data suggest that agriculture and urban development rates have accelerated. During the two sub-periods, the area of forest decreased and the ratio of the decrease between the two stages was about 40:1, showing that deforestation has slowed down in recent years.

The matrix of change gives knowledge of the main types of changes in the study area. Table 2 shows the matrix of land use and land cover change from 1987 to 2001. It can be found that forest cover decreased during the period 1987–2001. During the period 1987–2001, about 239.5 km^2

Table 1 | Results of land use and land cover classification for 1987, 2001 and 2007 images

Land use class	1987 Area (km^2)	%	2001 Area (km^2)	%	2007 Area (km^2)	%	Relative change area (km^2) 1987–2001	2001–2007	1987–2007
Grassland	1,641.79	66.93	1,722.26	70.21	1,636.89	66.73	80.47	−85.37	−4.9
Forest	665.01	27.11	509.73	20.78	505.81	20.62	−155.28	−3.92	−159.2
Barren land	108.91	4.44	160.43	6.54	155.27	6.33	51.52	−5.16	46.36
Farmland	29.44	1.2	48.32	1.97	118.97	4.85	18.88	70.65	89.53
Water body	2.70	0.11	6.62	0.27	5.64	0.23	3.92	−0.98	2.94
Residential land	5.15	0.21	5.64	0.23	30.42	1.24	0.49	24.78	25.27

Table 2 | Land use conversion matrix for 1987–2001 (km^2)

1987	2001 Grassland	Forest	Farmland	Barren land	Water body	Residential land	Total
Grassland	1,412.4	100.5	29.22	92.76	2.53	4.38	1,641.79
Forest	239.52	406.77	15.97	1.14	1.33	0.28	665.01
Farmland	23.89	1.92	2.79	0.39	0.36	0.09	29.44
Barren land	41.7	0.37	0.24	65.54	0.25	0.81	108.91
Water body	0.45	0.11	0.02	0	2.1	0.02	2.70
Residential land	4.3	0.06	0.08	0.6	0.05	0.06	5.15
Total	1,722.26	509.73	48.32	160.43	6.62	5.64	2,453

forest land was converted to grassland and 16.0 km^2 was converted to farmland. At the same time, forest land increased by 100 km^2 due to the conversion of grassland and conversion of 1.92 km^2 of farmland. During the same period, the increase in farmland was 29.2 km^2 from grassland and 0.24 km^2 from barren land. The matrices also indicated that increases in the barren land area mainly came from the grassland area, despite some barren land being converted to grassland.

The area of the grassland and forest decreased during the period 2001–2007, while the area of farmland and residential land obviously increased. From Table 3 it can be seen that the lost grassland was mainly converted to forest (149 km^2), farmland (92.6 km^2), barren land (62.4 km^2) and residential land (19.5 km^2). At the same time, 149 km^2 of forest was converted to grassland, 13.9 km^2 to farmland and 1.29 km^2 to residential land. The increase in residential land was mainly at the expense of grassland. The grassland, forest and barren land contributed to the increase in farmland during the same period.

In order to analyse the nature of land use and land cover changes, especially the area and spatial distribution of different land use and land cover changes, a set of 'gain' and 'loss' images for each category was also produced by integrating GIS and remote sensing (Figure 5; Weng 2002). From Figure 5, it can be seen that the net changes of forest area are larger than any other land use classes (Figure 5(a)). The change mainly occurred in the south of the study area and along the river. Many farmlands have been reclaimed recently, especially in the north part of the watershed (Figure 5(b)). Many new roads and irrigation channels were built during the study period. The increase in farmland and barren land occurred mainly in the northern part of the watershed. Compared with the land use and land cover map of 1987, it is found that these large changes were mainly due to the conversion of grassland. The vegetation degradation was obviously in the Shalamulun River watershed. Comparing Figures 5(b), (c) and (d), it can be seen that the increased farmland and barren land are mainly

Table 3 | Land use conversion matrix for 2001–2007 (km^2)

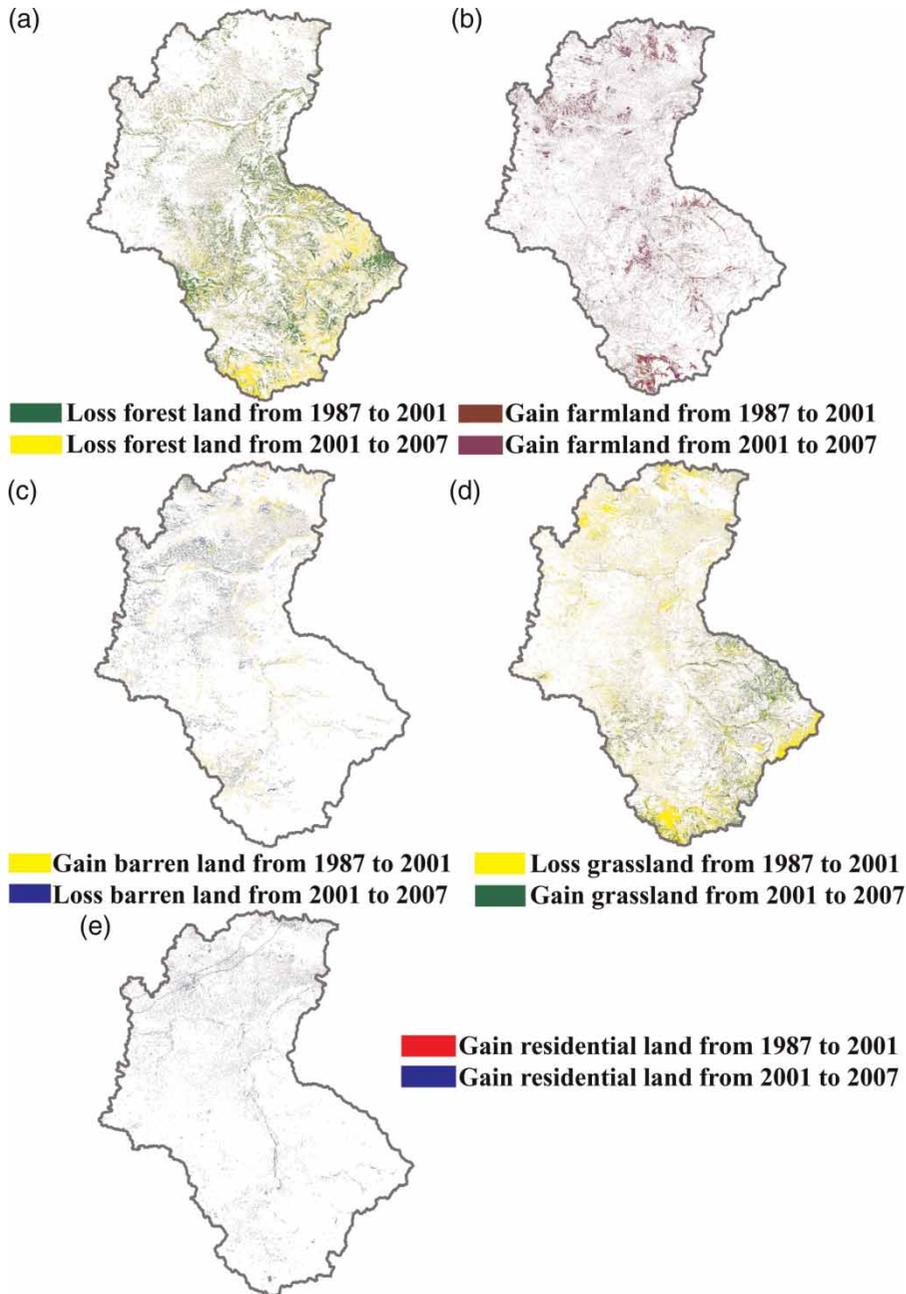| 2001	2007 Grassland	Forest	Barren land	Farmland	Residential land	Water body	Total
Grassland	1,398.34	148.55	62.43	92.61	19.54	0.79	1,722.26
Forest	149.22	345.04	0.1	13.92	1.29	0.16	509.73
Barren land	55.21	0.3	92.05	4.96	7.81	0.1	160.43
Farmland	30.48	10.25	0.12	7.16	0.3	0.01	48.32
Residential land	3.23	0.25	0.55	0.28	1.27	0.06	5.64
Water body	0.41	1.42	0.02	0.04	0.21	4.52	6.62
Total	1,636.89	505.81	155.27	118.97	30.42	5.64	2,453

Figure 5 │ Land use and land cover change during the period 1987–2001 and 2001–2007 of the land use classes: (a) forest; (b) farmland; (c) barren land; (d) grassland; and (e) residential land.

located around the residential land. This finding reveals that population growth, economical development (i.e. tourism) and development projects such as construction of infrastructural facilities (i.e. building of dam, irrigation channels, highways, etc.) are the main driving forces of the land use and land cover change.

Influence of land use and land cover on potential evapotranspiration

Mean annual PET for 1987, 2001 and 2007 were estimated by a two-source PET model (Figure 6). As shown in Figure 6, the spatial variation of mean annual PET over the watershed
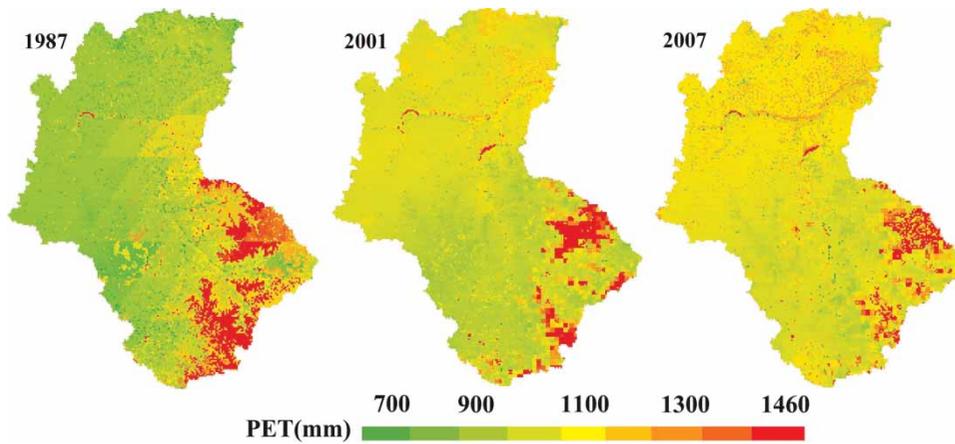
Figure 6 | Spatial distribution of annual PET of (a) 1987; (b) 2001; and (c) 2007 in the Shalamulun River watershed.

is non-uniform from 603 to 1,499 mm. Higher PET values occur in the river valley covered with water and the mountainous region covered with forest cover. Lower PET values mainly appear in the mid-north part of the watershed.

The mean monthly PET from 1987 to 2007, shown in Figure 7, varies from 10 mm (in January, November and December) to 123 mm (in July). The monthly PET is higher during growing seasons (i.e. from April to September) than other seasons, and the peak of monthly PET occurs in July. Most vegetation is considered to have only slight canopy coverage during winter months when it dies, but the coverage increases in spring through the summer. We therefore compared the monthly PET of the Shalamulun River watershed during growing seasons. Figure 8 shows that the PET value-has a temporal variation during growing seasons; the highest PET values of 92–242 mm are observed in July and the lowest of 55–150 mm in April and September. The mean PET value varies over 95–200 mm in June and August and over 90–195 mm in May. It can also be seen that the monthly
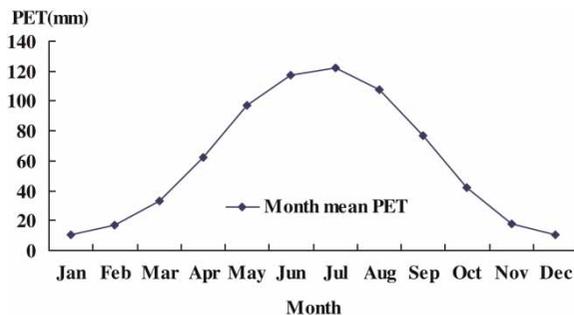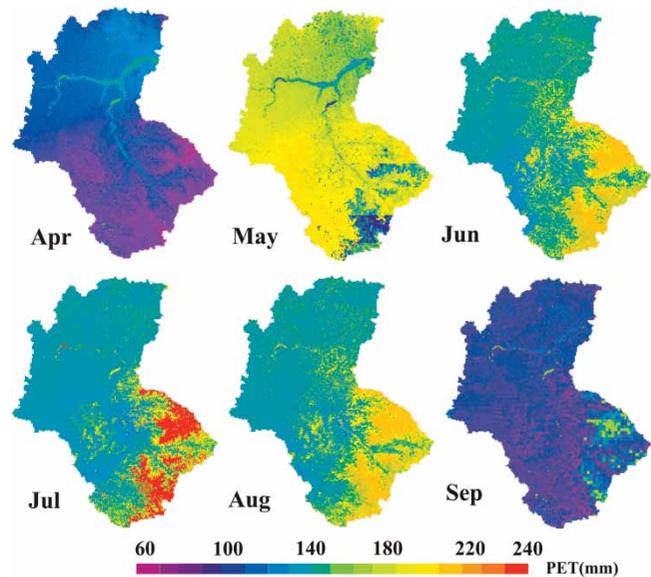

Figure 8 | Spatial distribution of PET during growing season from May to September in the Shalamulun River watershed from 1987 to 2007.

PET is spatially non-uniform for different land use types. Water bodies have very higher transpiration losses than other land covers throughout the growing seasons. The monthly PET of the forest cover is higher than other vegetation covers. The lowest monthly PET value is for grassland. It reflects that the land use and land cover classes have a significant influence on monthly PET.

Both climate change and land use and land cover changes can lead to the variations of PET. To quantify the influence of LUCC, PET was evaluated under the land use scenarios of 1987, 2001 and 2007, with the same

Figure 7 | Mean monthly PET of Shalamulun River watershed from 1987 to 2007.

meteorological record of 1987 (Figure 9). The total annual evapotranspiration losses for various land cover scenarios are given in Figure 9. From Figure 9 it can be seen that the mean annual PET decreased from 1987 to 2007 by about 20 mm, where the mean annual PET for 1987, 2001 and 2007 was 740, 723 and 713 mm, respectively. Figure 9 shows that the annual PET has decreased from 1987 to 2007 by 27 mm (from 740 to 713 mm). An initial comparison of the changes in annual PET of the two periods (1987–2001 and 2001–2007) shows that the annual PET of period 1 is 17 mm greater than annual PET in period 2 (5 mm). The change in annual PET is consistent with the changes in land use and land cover. The forest has a highly developed root system and a higher leaf area index so a much stronger hydraulic lift of water and transpiration than other vegetation types, leading to a higher PET value in 1987 than the other two years.

It is also found that annual PET is spatially heterogeneous for different land use types. The annual PET of forested land changed more than other land use types, with a decreasing value of 177 mm as the forest area decreased by about 159 km^2. The annual PET of farmland decreased by 45 mm while the area of farmland increased by about 89.5 km^2. For the increase in the barren land area of about 46.4 km^2, the annual PET of the barren land increased by about 26 mm. The annual PET of grassland decreased slightly (6 mm), especially during the study area.

It has been reported that a large change in PET did not occur, but the evaporative coefficient increased exponentially with LAI (Dunin & Mackay 1982; Zhang 1999). Figure 10 depicts the LAI of the main vegetation types in 1987 (Figure 10(a)), 2001 (Figure 10(b)) and 2007 (Figure 10(c)). It shows that the LAI of forest in growth season is higher than other vegetation types in three years, which contributed to the highest PET located on forest land.
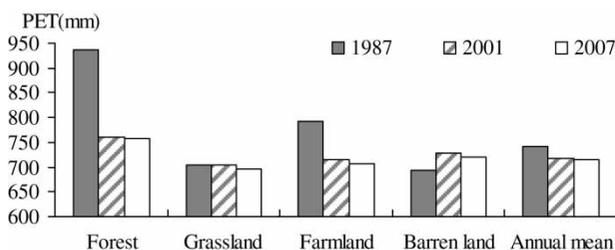

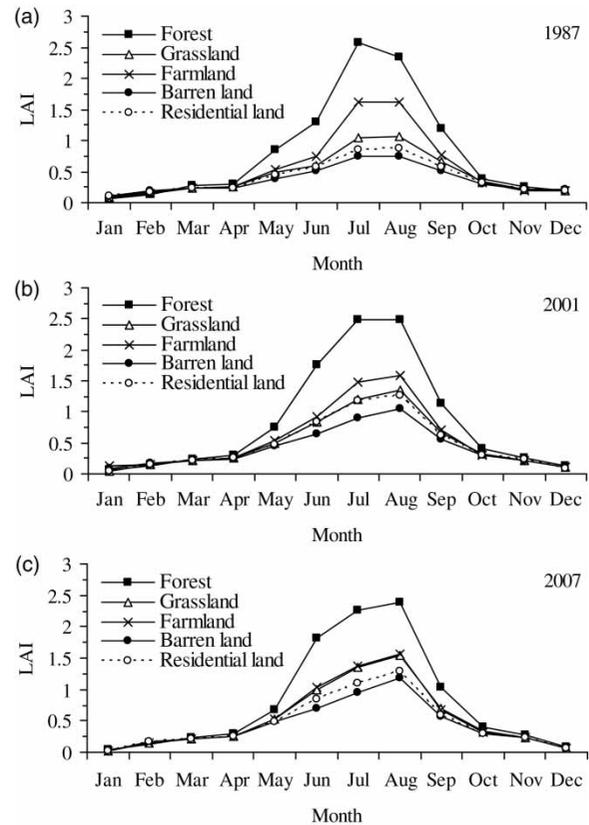**Figure 9** │ Annual PET on two land use scenarios for 1987, 2001 and 2007.

Figure 10 │ Mean monthly LAI for various land use class in (a) 1987; (b) 2001; and (c) 2007.

The LAI of farmland is higher than grassland; maize and helianthus are the main crop types, which have higher LAI during growing months than the grassland in 1987 and 2001. However, the LAIs of farmland and grassland are similar in 2007. This phenomenon can be explained by the fact that land use and land cover types for 2007 are derived from the TM image of October 7 2007. All crops were harvested at this time, leading to the misclassification of some cropland to grassland. As a key land surface biophysical parameter, LAI can reflect the land use and land cover class, especially during growing seasons (Turner *et al.* 1999). It shows that LUCC has a significant effect on the changes in PET.

Effect of changes in land use and land cover on the discharge of Shalamulun River

Both climate change and LUCC can lead to variations in annual runoff (Lu *et al.* 2008). Thus variations in annual precipitation series and observed runoff series were analysed.

Figure 11 shows that annual precipitation and runoff depth have a relative correlation from the late 1870s to early 1880s. However, during the period after 1998, annual runoff decreased dramatically while annual precipitation decreased only slightly. Land use and land cover changes may be one of the factors influencing the annual runoff decrease after 1998. Similar research demonstrates that the river discharge decreases more rapidly in semi-arid areas than other areas for the effect of land use and land cover changes (Ren *et al.* 2002).

For analysis of the effects of land use and land cover change on the discharge, we choose the method of Costa *et al.* (2003) to summarize the long-term means of the main surface hydrological components of the Shalamulun River watershed upstream of West Liao River for the three periods considered (Table 4). A decrease in precipitation of the order of 0.145 mm day^{-1} (52 mm yr^{-1} or 14%), a decrease in discharge of 0.086 mm day^{-1} (31 mm yr^{-1} or 35%), a decrease in ET of 0.059 mm day^{-1} (21 mm yr^{-1} or 7%) and a decrease in the runoff coefficient from 0.233 to 0.174 can be determined from Table 4. Compared to the decrease in precipitation, the 35% decrease in discharge is serious in semi-arid regions. That is to say, the lower long-term discharge and lower runoff coefficient are consistent with the land use and land cover changes.
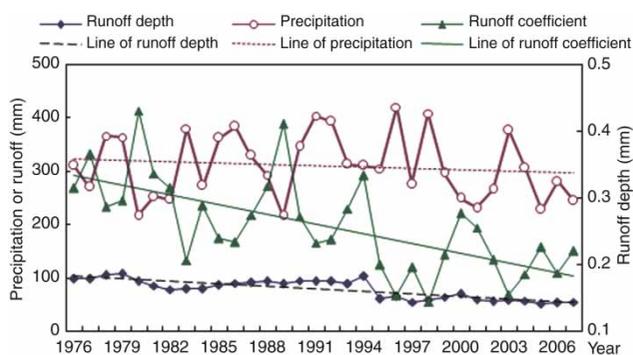

Figure 11 │ Variation of annual precipitation, observed runoff and runoff coefficient at Henanyingzi Station in Shalamulun River watershed from 1976 to 2007.

CONCLUSIONS

In this study, an attempt is made to quantitatively assess the effect of land use and land cover changes on PET and runoff in the Shalamulun River watershed by a two-source PET model and statistical analysis supported by RS and GIS techniques. This study analyses the classification of land use and land cover in the Shalamulun River watershed in Inner Mongolia.

Land use and land cover changes in the watershed were analysed for three periods over the period 1987–2007. Spatio-temporal variations of the land use types were analysed using the spatial analysis algorithm in the ArcGIS 9.2. These results provide a perspective on land use and land cover classes and their changes that have taken place. From 1987 to 2007, the forest land in the study area has decreased to varying degrees; however, residential land, barren land and farmland have increased during the same period.

The general trends of LUCC are as follows. Forest land and grassland are mainly converted to farmland and residential land. Land degradation, especially deforested and developing cultivated land, are the main reasons for regional environmental deterioration. In semi-arid regions, the ecological environment is highly sensitive to climate change and human activities. Consequently, vulnerable areas have suffered serious degradation and the relationship between man and land is important.

At the headwater of West Liao River, the river watershed had been exploited during the ninth five-year development plan for national economic and social development. During this period, the Chinese land use policy has changed greatly, affecting the land use change of the study basin. An increase in residential areas and barren land and a decrease in grassland and crop land as a result of tourism or development projects (e.g. building of dams, highways, etc.) are evident. Natural driving forces such as topography, slope and soil conditions are unimportant for land use change in the

Table 4 │ Long-term mean of hydrological variables in the Shalamulun River watershed

Period	Precipitation *P* (mm day^{-1})	Discharge *Q* (mm day^{-1})	Evapotranspiration ET (mm day^{-1})	Runoff coefficient (*Q/P*)
1978–1987	1.045	0.243	0.802	0.233
1998–2007	0.9	0.157	0.743	0.174

Shalamulun River watershed. Otherwise, human activity is the major force in shaping the land use change.

Annual PET varies spatially for different types of land use and land cover in Shalamulun River watershed. The monthly PET value has a spatio-temporal variation during the growing seasons (i.e. from April to September). The results reveal that the land use and land cover classes and changes have a significant influence on PET. Meanwhile, both annual PET and runoff decrease with decreasing grassland and increasing farmland. Thus, land use and land cover changes have a significant impact on the hydrological cycle. In semi-arid regions, a decrease in discharge can deteriorate the aquatic ecological environment and make water supply difficult for domestic and agricultural purposes (Ren *et al.* 2002). These results should be the focus of water managers and ecologists.

The conversion of vegetation such as forest to farmland or grassland disrupts the hydrological cycle of a watershed by altering the balance between rainfall and evaporation and consequently the runoff response of the area (Costa *et al.* 2003). The analysis presented here indicates that although precipitation changed very little during the study period, annual mean discharge reduced by 35%. Increased infiltration and decreased precipitation contributes to reduced runoff. The changes in land use and land cover cause an increase in infiltration and a decrease in surface flow.

In this study, only PET and runoff are used to analyse the effect of land use and land cover changes. The impacts of land use and land cover changes on hydrological regimes, however, are not easy to quantify because they are the result of interplay between various hydrological processes such as climatic factors, vegetation characteristics, site-specific conditions and management factors (Conway 2001). In the future, more work needs to be done to quantify the relationship of land use and land cover changes applying to a hydrologic model to field studies of land use and land cover changes.

ACKNOWLEDGEMENTS

REFERENCES

Bach, M., Breuer, L., Frede, H. G., Huisman, J. A., Otte, A. & Waldhardt, R. 2006 Accuracy and congruency of three different digital land-use maps. *Landscape Urban Plan.* **78**, 289–299.

Bellot, J., Bonet, A., Sanchez, J. R. & Chirino, E. 2001 Likely effect of land use changes on the runoff and aquifer recharge in a semiarid landscape using a hydrological model. *Landscape Urban Plan.* **55**, 41–53.

Benediktsson, J. A., Swain, P. H. & Ersoy, O. K. 1990 Neural network approaches versus statistical methods in classification of multisource remote sensing data. *IEEE T. Geosci. Remote* **28** (4), 540–551.

Berberoglu, S. & Akin, A. 2009 Assessing different remote sensing techniques to detect land use/cover changes in the eastern Mediterranean. *Int. J. Appl. Earth Observ. Geoinform.* **11** (1), 46–53.

Brodley, C. E. & Utgoff, P. E. 1992 *Multivariate Versus Univariate Decision Trees*. Technical Report 92-8. University of Massachusetts, Amherst, MA, USA.

Chavez, P. S. 1996 Image-based atmospheric corrections revisited and improved. *Photogram. Eng. Remote Sens.* **62**, 1025–1036.

Cohena, Y. & Shoshany, M. 2005 Analysis of convergent evidence in an evidential reasoning knowledge-based classification. *Remote Sens. Environ.* **96** (3–4), 518–528.

Congalton, R. G. & Green, K. 1999 *Assessing the Accuracy of Remotely Sensed Data: Principles and Practices*. Florida Lewis Publishers, Boca Rotan, 43–64.

Conway, D. 2001 Understanding the hydrological impacts of land cover and land use change. *IHDP Update* **1**, 5–6.

Costa, M. H., Botta, A. & Cardille, J. A. 2003 Effects of large-scale changes in land cover on the discharge of the Tocantins River, Southeastern Amazonia. *J. Hydrol.* **283**, 206–217.

DeFries, R. S., Hansen, M. C., Townshend, J. R. G. & Sohlberg, R. S. 1998 Global land cover classifications at 8 km spatial

resolution: the use of training data derived from Landsat imagery in decision tree classifiers. *Int. J. Remote Sens.* **19**, 3141–3168.

Dewan, A. M. & Yamaguchi, Y. 2009 Land use and land cover change in Greater Dhaka, Bangladesh: using remote sensing to promote sustainable urbanization. *Appl. Geogr.* **29** (3), 1–12.

Diouf, A. & Lambin, E. F. 2001 Monitoring land-cover changes in semi-arid regions: remote sensing data and field observations in the Ferlo, Senegal. *J. Arid Environ.* **48** (2), 129–148.

Dunin, F. X. & MacKay, S. M. 1982 *Evaporation of eucalypt and coniferous forest communities.* First National Symposium on Forest Hydrology, Melb. 18–25.

Fohrer, N., Haverkamp, S., Eckhardt, K. & Frede, H. G. 2001 Hydrologic response to land use changes on the catchment scale. *Phys. Chem. Earth.* (B). **26** (7–8), 577–582.

Govers, G., Oost, K. V. & Poesen, J. 2006 Responses of a semi-arid landscape to human disturbance: a simulation study of the interaction between rock fragment cover, soil erosion and land use change. *Geoderma.* **133** (1–2), 19–31.

Hathout, S. 2002 The use of GIS for monitoring and predicting urban growth in East and West St Paul, Winnipeg, Manitoba, Canada. *J. Environ. Manage.* **66**, 229–238.

Hégarat-Mascle, S. L., Blochm, I. & Vidal-Madjar, D. 1997 Application of Dempster–Shafer evidence theory to unsupervised classification in multisource remote sensing. *IEEE T. Geosci. Remote.* **35**, 1018–1031.

Hovius, N. 1998 Controls on sediment supply by large rivers, relative role of Eustasy, climate, and tectonism in continental rocks. *Society of Sedimentary Geology* **59**, 3–16 (Special Publication).

Kandrika, S. & Roy, P. S. 2008 Land use land cover classification of Orissa using multi-temporal IRS-P6 awifs data: a decision tree approach. *Int. J. Appl. Earth Observ. Geoinform.* **10** (2), 186–193.

Lambin, E. F., Geist, H. & Lepers, E. 2003 Dynamics of land use and cover change in tropical regions. *Ann. Rev. Environ. Res.* **28**, 205–241.

Langley, S. K., Cheshire, H. M. & Humes, K. S. 2001 A comparison of single date and multitemporal satellite image classifications in a semi-arid grassland. *J. Arid. Environ.* **49**, 401–411.

Liu, J. Y. 1996 *The Macro Investigation and Dynamic Research of the Resource and Environment.* China Science and Technology Press, Beijing.

Lu, D. S., Mausel, P., Batistella, M. & Moran, E. 2005 Land-cover binary change detection methods for use in the moist tropical region of the Amazon: a comparative study. *Int. J. Remote Sens.* **26**, 101–114.

Lu, G. B., Li, Q. F., Zou, Z. H., Wang, H. J., Xia, Z. Q. & Ma, X. R. 2008 Impact of human activities on the flow regime of the Yellow River. In: *Hydrological Sciences for Managing Water Resources in the Asian Developing World* (X. H. Chen, Y. Q. Chen J. Xia & H. L. Zhang, eds.). Proceedings of Symposium

in Guangzhou, China, June 2006, pp. 184–191. IAHS Press, Wallingford, UK.

Lucas, I. F. J., Frans, J. M. & Wel, V. D. 1989 Accuracy assessment of satellite derived land-cover data: a review. *Photogramm. Eng. Rem. S.* **10** (6), 1310–1317.

Mo, X. G., Liu, S., Liu, Z. & Zhao, W. 2004 Simulating temporal and spatial variation of evapotranspiration over the Lushi basin. *J. Hydrol.* **285**, 125–142.

Pal, M. & Mather, P. M. 2003 An assessment of the effectiveness of decision tree methods for land cover classification. *Remote Sens. Environ.* **86** (4), 554–565.

Peddle, D. R. 1995 Knowledge formulation for supervised evidential classification. *Photogram. Eng. Remote Sens.* **61** (4), 409–417.

Pontius, R. H., Boersma, W., Castella, J. C., Clarke, K., de Nijs, T., Dietzel, C., Duan, Z., Fotsing, E., Goldstein, N., Kok, K., Koomen, E., Lippitt, C., McConnell, W., Mohd, S. A., Pijanowski, B., Pithadia, S., Sweeney, S., Trung, T., Veldkamp, A. & Verburg, P. H. 2008 Comparing the input, output, and validation maps for several models of land change. *Ann. Regional Sci.* **42**, 11–37.

Ren, L. L., Liu, X. F., Yuan, F., Singh, V. P., Fang, X. Q., Yu, Z. B. & Zhang, W. 2009 Quantitative effect of land use and land cover change on green water and blue water in northern part of China. In: *Hydrological Changes and Watershed Management from Headwaters to the Ocean* (M. Taniguchi, W. C. Burnett & Y. Fuku, eds.). Taylor & Francis Group, London, pp. 187–193.

Ren, L. L., Wang, M. R., Li, C. H. & Zhang, W. 2002 Impacts of human activity on river runoff in the north area of China. *J. Hydrol.* **261**, 204–217.

Richards, J. A. 1992 *Remote Sensing Digital Image Analysis.* Springer-Verlag, Cambridge, UK.

Serra, P., Pons, X. & Saur, D. 2008 Land-cover and land-use change in a Mediterranean landscape: a spatial analysis of driving forces integrating biophysical and human factors. *Appl. Geogr.* **28**, 189–209.

Sesnie, S. E., Gessler, P. E., Finegan, B. & Thesslerm, S. 2008 Integrating Landsat TM and SRTM-DEM derived variables with decision trees for habitat classification and change detection in complex neotropical environments. *Remote Sens. Environ.* **112**, 2145–2159.

Shafer, G. 1976 *A Mathematical Theory of Evidence.* Princeton University Press, New Jersey.

Shalaby, A. & Tateishi, R. 2007 Remote sensing and GIS for mapping and monitoring land cover and land-use changes in the Northwestern coastal zone of Egypt. *Appl. Geogr.* **7** (1), 28–41.

Stefanov, W. L., Michael, S. R. & Philip, R. 2001 Christensen Monitoring urban land cover change: an expert system approach to land cover classification of semiarid to arid urban centers. *Remote Sens. Environ.* **77** (2), 173–185.

Stehman, S. V. & Czaplewski, R. L. 1998 Design and analysis for thematic map accuracy assessment: fundamental principles. *Remote Sens. Environ.* **64**, 331–344.

Stow, D. A. 1999 Reducing mis-registration effects for pixel-level analysis of land-cover change. *Int. J. Remote Sens.* **20**, 2477–2483.

Turner, D. P., Cohen, W. B., Kennedy, R. E., Fassnacht, K. S. & Briggs, J. M. 1999 Relationships between leaf area index and Landsat tm spectral vegetation indices across three temperate zone sites. *Remote Sens. Environ* **70**, 52–68.

Verburg, P. H., Van de Steeg, J., Veldkamp, A. & Willemen, L. 2009 From land cover change to land function dynamics: a major challenge to improve land characterization. *J. Environ. Manage.* **90** (3), 1327–1335.

Wei, W., Wu, D. P., Gui, L. D., Chen, L. D., Fu, B. J. & Huang, Z. L. 2007 The effect of land uses and rainfall regimes on runoff and soil erosion in the semi-arid loess hilly area, China. *J. Hydrol.* **335** (3–4), 247–258.

Weng, Q. H. 2002 Land use change analysis in the Zhujiang Delta of China using satellite remote sensing, GIS and stochastic modeling. *J. Environ. Manage.* **64**, 273–284.

Wharton, S. W. 1989 Knowledge-based spectral classification of remotely sensed image data. In: *Theory and Applications of Optical Remote Sensing* (G. Asrar, ed.). Wiley, New York.

Winnaar, G. D., Jewitt, G. P. W. & Horan, M. 2007 A GIS-based approach for identifying potential runoff harvesting sites in the Thukela River basin, South Africa. *Phys. Chem. Earth.* **32**, 1058–1067.

Xiao, J. Y., Shen, Y. J., Ge, J. F., Tateishi, R., Tang, C. Y., Liang, Y. Q. & Huang, Z. Y. 2006 Evaluating urban expansion and land use change in Shijiazhuang China, by using GIS and remote sensing. *Landscape Urban Plan.* **75**, 69–80.

Yuan, F., Ren, L. L., Yu, Z. B. & Xu, J. 2008 Computation of potential evapotranspiration using a two-source method for the Xin'anjiang Hydrological model. *J. Hydraul. Eng.* **13** (5), 305–316.

Yuan, F., Sawaya, K. E., Loeffelholz, B. C., Marvin, E. & Bauer, M. E. 2005 Land cover classification and change analysis of the Twin Cities (Minnesota) Metropolitan Area by multitemporal Landsat remote sensing. *Remote Sens. Environ.* **98**, 317–328.

Zhang, B. P., Yao, Y. H., Cheng, W. M., Zhou, C. H., Lu, Z. & Chen, X. D. 2002 Human-induced changes to biodiversity and alpine pastureland in the Bayanbulak Region of the East Tianshan Mountains. *Mt. Res. Dev.* **22**, 1–7.

Zhang, L., Dawes, W. R. & Walker, G. R. 1999 Predicting the effect of vegetation changes on catchment average water balance. CRC for Catchment Hydrology Technical Report. 99/12. 1999.

Zhao, C. Y., Nan, Z. R. & Feng, Z. D. 2004 GIS-assisted spatially distributed modeling of the potential evapotranspiration in semiarid climate of the Chinese Loess Plateau. *J. Arid Environ.* **58**, 387–403.